Proc. Natl. Acad. Sci. USA
Vol. 92, pp. 9593–9597, October 1995
Biophysics

min K channels form by assembly of at least 14 subunits

T. TZOUNOPOULOS*†, H. R. GUY‡, S. DURELL‡, J. P. ADELMAN*†, AND J. MAYLIE§¶

*Vollum Institute and Departments of †Molecular and Medical Genetics and §Obstetrics and Gynecology, Oregon Health Sciences University, 3181 S.W. Sam Jackson Park Road, Portland, OR 97201; and ‡Laboratory of Mathematical Biology, National Institutes of Health, Bethesda, MD 20892

Communicated by Bertil Hille, University of Washington, Seattle, WA, June 27, 1995 (received for review March 6, 1995)

ABSTRACT **Injection of min K mRNA into *Xenopus* oocytes results in expression of slowly activating voltage-dependent potassium channels, distinct from those induced by expression of other cloned potassium channels. The min K protein also differs in structure, containing only a single predicted transmembrane domain. While it has been demonstrated that all other cloned potassium channels form by association of four independent subunits, the number of min K monomers which constitute a functional channel is unknown. In rat min K, replacement of Ser-69 by Ala (S69A) causes a shift in the current–voltage (*I–V*) relationship to more depolarized potentials; currents are not observed at potentials negative to 0 mV. To determine the subunit stoichiometry of min K channels, wild-type and S69A subunits were coexpressed. Injections of a constant amount of wild-type mRNA with increasing amounts of S69A mRNA led to potassium currents of decreasing amplitude upon voltage commands to −20 mV. Applying a binomial distribution to the reduction of current amplitudes as a function of the different coinjection mixtures yielded a subunit stoichiometry of at least 14 monomers for each functional min K channel. A model is presented for how min K subunits may form a channel.**

The min K protein was originally cloned from rat kidney (1), and min K mRNA has subsequently been detected in other tissues, including heart, uterus, lymphocytes, and submandibular gland (2–4). When expressed in *Xenopus* oocytes, the min K protein forms a slowly activating voltage-dependent potassium channel, different from other cloned potassium channels (1, 5, 6). In addition, min K displays no structural homology to other cloned potassium channels (7–13), suggesting that the min K protein may not form a channel, but act as an inducer of otherwise silent channels (14). However, point mutations within the predicted transmembrane domain (TM) of min K resulted in alterations of conduction and pore properties (15) supporting the hypothesis that the min K protein does indeed form potassium-selective channels (16).

Other voltage-gated and inward rectifier potassium channels form by the coassembly of four independent subunits (17–20). The different structural and functional features of min K suggest a distinct subunit stoichiometry for min K channels. The results presented here demonstrate that coexpression of wild-type min K subunits with subunits containing a point mutation, Ser-69 → Ala (S69A), which imparts significantly different voltage dependence and kinetics, allowed an estimate of at least 14 min K monomers per functional channel.

METHODS

Site-directed mutagenesis, *in vitro* mRNA synthesis, and oocyte injections were performed as previously described (21). To control mRNA concentrations, plasmid DNAs were prepared in parallel and spectrophotometrically quantified. The DNAs were mixed in appropriate ratios (see *Results*) prior to transcription, and mRNA synthesis was performed using common pools of reagents. After synthesis, mRNAs were spectrophotometrically quantified. *Xenopus* care and handling were as previously described (6). Two to 5 days after mRNA injection, macroscopic currents were measured by using a two-electrode voltage clamp with a CA-1 amplifier interfaced to an LSI 11/73 computer. Data were filtered at 1 kHz and sampled at 50 Hz. During recording, oocytes were continuously superfused with ND-96 (96 mM NaCl/2 mM KCl/1.8 mM $CaCl_2$/1 mM $MgCl_2$/5 mM Hepes, pH 7.6) at room temperature.

The subunit stoichiometry of min K was determined from the binomial theorem applied to the relative current amplitudes for different coinjection mixtures. For a random assembly of subunits the relative current amplitude is given by

$$\sum_{i=0}^{n} C_i^n \cdot x^{n-i} \cdot (1-x)^i,$$

where x = the fraction of wild-type subunits, n = subunit stoichiometry, and $C_i^n = n!/i!(n-i)!$. For a single subunit sufficient to alter channel function $i = 0$. All data are expressed as mean ± SD.

RESULTS

Expression of Wild-Type and Mutant min K Channels. Depolarizing voltage commands delivered to *Xenopus* oocytes injected with wild-type min K mRNA evoked slowly activating voltage-dependent potassium currents not present in noninjected oocytes. Channel kinetics and voltage dependence of activation were examined. Fitting the rising phase of the current traces at 20 mV with the sum of two exponentials (Fig. 1*A*) yielded activation time constants of τ_{fast} = 3.5 ± 0.5 s and τ_{slow} = 26 ± 1.3 s with relative amplitudes of 0.27 and 0.73, respectively (n = 5). After repolarization to −60 mV the channels deactivated with a time course which was best fitted by the sum of two exponential functions, yielding time constants of τ_{fast} = 0.55 ± 0.1 s and τ_{slow} = 3.0 ± 0.4 s, with relative amplitudes of 0.5 for each component (n = 5). Voltage dependence of activation was determined by applying a Boltzmann function to the instantaneous tail currents as a function of test potential between −60 and 40 mV; a double-exponential was fitted to tail currents and extrapolated to the beginning of the tail pulse. The voltage for half-maximal activation, $V_{1/2}$, was −8 ± 2 mV and the slope factor, k, was 12.4 ± 0.3 mV (n = 5; Table 1).

Ser-69 is predicted to reside at the cytoplasmic border of the transmembrane domain. Introduction of S69A in rat min K resulted in altered voltage dependence and kinetics at potentials between −60 and 40 mV (Fig. 1*B*). Activation kinetics of S69A channels examined by fitting a sum of two exponentials to the rising phase of the current trace at 20 mV (Fig. 1*B*) yielded time constants that were decreased compared with wild-type channels, τ_{fast} = 2.1 ± 0.1 s and τ_{slow} = 20.3 ± 1 s, and relative amplitudes of 0.36 and 0.64, respectively (n = 5).

The publication costs of this article were defrayed in part by page charge payment. This article must therefore be hereby marked "*advertisement*" in accordance with 18 U.S.C. §1734 solely to indicate this fact.

¶To whom reprint requests should be addressed.

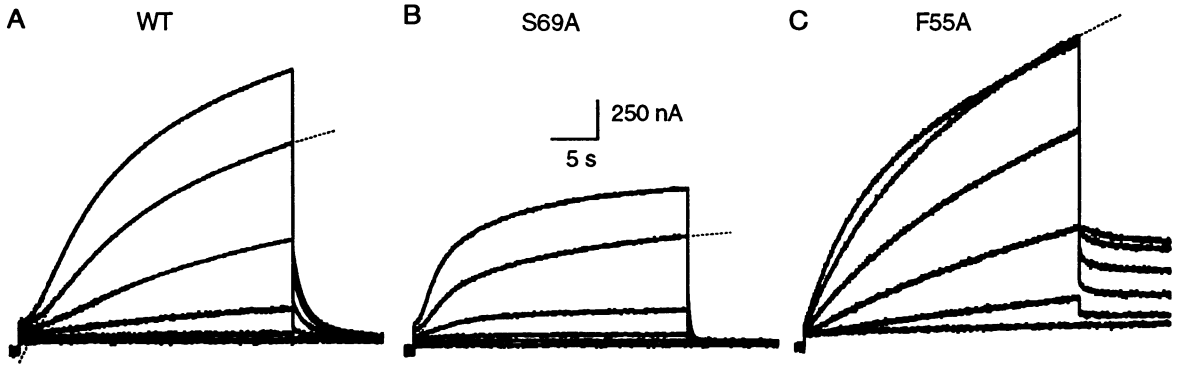

FIG. 1. Expression of wild-type and mutant min K channels. Current records are from oocytes expressing wild-type min K channels (*A*), S69A min K channels (*B*), and F55A min K channels (*C*). From a holding potential of −80 mV, currents were elicited by 30-s depolarizing commands to potentials from −60 to 40 mV in 20-mV increments followed by repolarization to a tail potential of −60 mV. The traces at 20 mV are presented with fits of a double-exponential function. For the traces presented in *C*, a 10-s prepulse to −120 mV was applied prior to depolarization. The initial jump apparent in some records is due to an endogenous chloride current. For wild type and F55A, 5 ng of mRNA was injected; for S69A, 50 ng of mRNA was injected.

Deactivation kinetics were also significantly faster than those of wild-type channels; τ_{fast} = 0.24 ± 0.05 s and τ_{slow} = 1.9 ± 0.1 s, and relative amplitudes of 0.88 and 0.12, respectively (n = 5). The Boltzmann parameters of S69A channels revealed a shift to more positive potentials, $V_{1/2}$ = 15 ± 2 mV and k = 9.4 ± 0.3 mV (n = 5; Table 1). Indeed, currents from oocytes expressing S69A are detected only at potentials positive to 0 mV; no currents could be detected at −20 mV. This made analysis of S69A currents difficult due to contamination by endogenous sodium channels which are activated at potentials positive to 20 mV.

Another point mutation was also examined. Phenylalanine at position 55 was replaced by alanine (F55A); this residue is predicted to reside within the transmembrane domain. Expression of this mutant resulted in current amplitudes not different from wild type (Fig. 1*C*). However, activation kinetics were altered, with τ_{fast} = 5.6 ± 0.5 s and τ_{slow} = 38.5 ± 1.3 s, and relative amplitudes of 0.15 and 0.85, respectively (n = 5). Deactivation kinetics at −60 mV yielded time constants that were larger than wild type, τ_{fast} = 2.5 ± 0.2 s and τ_{slow} = 4.4 ± 0.4 s, with relative amplitudes of 0.49 and 0.51, respectively (n = 5). The voltage dependence of F55A channels was shifted to more negative potentials compared with wild type; $V_{1/2}$ = −26 ± 2 mV and k = 13.4 ± 0.3 mV (n = 5) (Table 1). Thus, compared with wild-type channels the substitution F55A shifted voltage dependence to more negative potentials, and tail currents for all test potentials deactivated significantly slower than wild type.

min K Channels Are Composed of Multimers of min K Monomers. To test whether min K channels are composed of multimers of min K monomers, wild-type and mutant subunits were coexpressed. Equal amounts of DNA were linearized and mRNAs were synthesized using common pools of reagents; *in vitro* synthesized mRNAs were also qualitatively and quantitatively evaluated (see *Methods*). In addition, it has been previously shown that S69A and wild-type mRNAs produce equal amounts of membrane-bound min K subunits (22). Fig. 2 shows current families after coinjection of a constant amount of wild-type mRNA together with water (*A*) or various amounts of S69A mRNA (*B–D*). Coinjected oocytes displayed reduced current amplitudes compared to wild type at all potentials tested. The current amplitude reduction demonstrates that S69A subunits have a dominant negative effect on coexpressed wild-type subunits, suggesting that wild-type and S69A subunits coassemble. Complementary results were obtained when a constant amount of F55A was coinjected with various amounts of wild type (not shown). In this case, the voltage dependence of the mutant is shifted to more negative potentials, resulting in decreased current amplitudes at potentials below −40 mV due to dominant negative effects of wild-type subunits, while at more positive potentials the current amplitudes are increased due to the additional contribution of channels composed of either wild-type subunits or wild-type and F55A subunits. Therefore, min K channels are composed of more than one subunit.

Subunit Stoichiometry of Functional min K Channels. As discussed above, coinjection of increasing amounts of S69A mRNA with a constant amount of wild-type mRNA resulted in current amplitudes that were smaller than wild type alone. To assess the subunit stoichiometry of min K channels in oocytes injected with different ratios of wild-type and S69A mRNAs, a binomial distribution was applied to tail current amplitudes at −60 mV following a test pulse to −20 mV. The analysis presented below assumes that (*i*) wild-type and mutant channels express equally, (*ii*) the different subunits assemble randomly, and (*iii*) one S69A subunit abolishes channel function at −20 mV. At this voltage, channel kinetics from all coinjection mixtures were indistinguishable from wild type, suggesting that only wild-type channels contribute to the current at −20 mV (Table 2). In contrast, channel kinetics following test pulses to 20 mV showed increasing rates of deactivation at −60 mV as the amount of S69A mRNA was

Table 1. Kinetic characteristics and voltage dependence of wild-type (WT), S69A, and F55A channels

	Activation					Deactivation		
Channel	τ_{fast}, s	τ_{slow}, s	A_f	$V_{1/2}$, mV	k, mV	τ_{fast}, s	τ_{slow}, s	A_f
WT	3.5 ± 0.5	26.0 ± 1.3	0.27	−8 ± 2	12.4 ± 0.3	0.5 ± 0.1	3.0 ± 0.4	0.50
S69A	2.1 ± 0.1	20.3 ± 1.0	0.36	15 ± 2	9.4 ± 0.3	0.2 ± 0.05	1.9 ± 0.1	0.88
F55A	5.6 ± 0.5	38.5 ± 1.3	0.15	−26 ± 2	13.4 ± 0.3	2.5 ± 0.2	4.4 ± 0.4	0.50

Activation kinetics were examined by fitting a sum of two exponentials to the rising phase of the current trace at 20 mV. After repolarization to −60 mV, the channel deactivation time course was fit by a sum of two exponentials. Voltage dependence of activation was determined by applying a Boltzmann function, $1/(1 + e^{-(V-V_{1/2})/k})$, to the instantaneous tail current as a function of test potential between −60 and 40 mV. A_f is the relative contribution of the fast component; n = 5 for all measurements; errors are SD.

increased, suggesting that channels composed of both wild-type and S69A subunits contribute to the current at 20 mV. Current traces evoked by test pulses to −20 mV and 20 mV from oocytes injected with a constant amount of wild-type plus various amounts of S69A mRNAs are presented in Fig. 3*A* and *C*, respectively. The difference in kinetics is apparent from the tail currents; these are presented, with double-exponential fits, in Fig. 3*B* (after test pulses to −20 mV) and 3*D* (after test pulses to 20 mV). To determine the minimum number of min K subunits which assemble to form the channel, tail current amplitudes after test pulses to −20 mV from the various mixtures were plotted as a function of the ratio of wild-type to S69A mRNA. The data points were fitted to the first term of the binomial expression (Fig. 3*E*). The data were best fit when $n = 13.7$, suggesting that at least 14 min K monomers assemble to form functional channels (Fig. 3*E*). For comparison, curves for $n = 10$ and $n = 18$ are also shown.

Analogous experiments were performed using oocytes coinjected with a constant amount of F55A and various amounts of wild-type mRNAs. As the amount of wild-type mRNA was increased, the tail current amplitudes at −60 mV after a test pulse to −40 mV were reduced compared with oocytes injected with F55A mRNA alone, and the tail current retained the kinetic characteristics of F55A. Analysis of the current amplitude reduction as a function of the different coinjection mixtures yielded an estimate of at least 14 subunits per functional channel, in agreement with the results independently obtained from coinjections of wild-type and S69A mRNAs.

DISCUSSION

To assess the subunit composition of min K channels, the effects of coexpressing wild-type min K and a point mutant, S69A, were studied. Although S69A and wild-type subunits are equally expressed (21), current amplitudes from oocytes expressing only S69A are much reduced compared with wild type at potentials between −60 and 40 mV. This is, at least in part, due to the shifted voltage dependence of S69A compared with wild type; measurable currents are observed only at potentials positive to 0 mV.

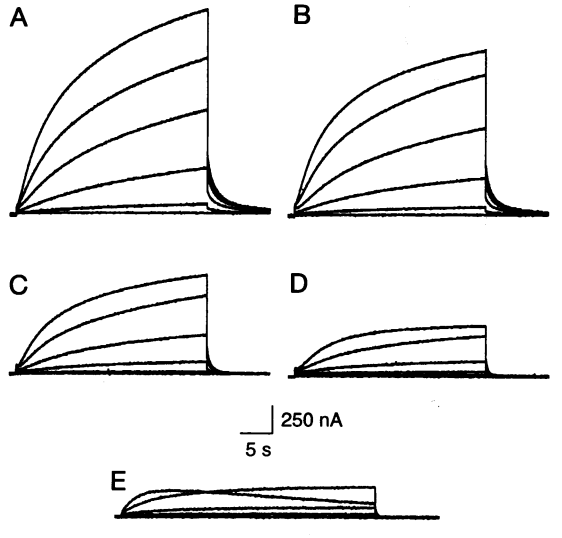

FIG. 2. Current families induced by injection of wild-type and S69A mRNAs. (*A*) Current records from an oocyte injected with only wild-type mRNA (5 ng). (*B–D*) Currents recorded after coinjection of a constant amount of wild-type mRNA (5 ng) with various amounts of S69A mRNA (relatively, 0.01, 0.1, or 1 in *B*, *C*, and *D*, respectively). (*E*) Current records from an oocyte injected with only S69A mRNA (5 ng). Voltage protocols are the same as in Fig. 1 *A* and *B*.

To determine whether min K channels are composed of more than one monomer, and to estimate the subunit stoichiometry of min K channels, the differences in voltage dependence and kinetics between wild-type and S69A channels were exploited. Injecting a constant amount of wild-type mRNA with increasing amounts of S69A mRNA led to decreased potassium currents at all potentials tested, suggesting that the two different kinds of subunits coassemble. In addition, the kinetics of the current at −20 mV are indistinguishable from wild type, while at more depolarized potentials the kinetics are not consistent with channels composed only of wild-type or S69A subunits. Thus, injection of mixtures of wild-type and S69A mRNAs results in a heterogeneous population of channels with relative proportions reflecting a binomial distribution and the exponent equal to the subunit stoichiometry of the channel. At −20 mV only the subpopulation composed of all wild-type subunits can pass ions. Application of the binomial distribution to the decrease in wild-type tail current amplitudes after commands to −20 mV yielded a value of 14 min K monomers per functional min K channel. This result is based on three assumptions. The first assumption is that wild-type and mutant channels express equally. Takumi *et al.* (22) used immunoprecipitations to determine the relative amount of wild-type and S69A subunits in *Xenopus* oocyte membranes and found little if any difference. The second assumption is that wild-type and mutant subunits assemble randomly. This is supported by the data from oocytes injected with equal amounts of wild-type and S69A mRNAs; at −20 mV no current was detected. If wild-type or S69A subunits more readily formed homo- rather than heteromeric complexes, then some wild-type channel activity would be expected. Further, identical estimates for min K subunit stoichiometry were obtained when F55A, a mutation residing within a different region of the subunit, was used. The third assumption is that only homomeric wild-type channels pass current at −20 mV; one or more S69A subunits alter channel function such that they cannot pass current at this potential. This is suggested by the finding that, regardless of the amount of S69A mRNA coinjected with wild-type mRNA, the activation and deactivation rates of the current elicited at −20 mV are indistinguishable from wild type. Further, the data points are best fit when constrained to this assumption. The fit is much poorer when modified to assume that two or more S69A subunits are required to alter channel function. If two or more S69A subunits are required, then the coefficient, n, would necessarily become larger and the number of subunits per functional min K channel would increase (Fig. 3*F*). For instance, if two S69A subunits are required for inhibition at −20 mV, then the subunit stoichiometry would be 26; this is not compatible with the data. However, we cannot exclude that one S69A subunit may cause partial inhibition while two result in complete inhibition; n would then be between 14 and 36 (see below).

The finding that min K channels are composed of at least 14 subunits is in contrast to the other known potassium channel families in which the subunit stoichiometry is 4 (18, 24). The dashed curve in Fig. 3*E* shows the predicted fit if four min K subunits make a functional channel; the data do not support this stoichiometry.

How might such a molecule form an ion channel? When channels are formed by identical subunits, it is generally assumed that the subunits have the same conformation and are related by radial symmetry about the axis of the pore. If min K channels are formed by assembly of at least 14 identical subunits, they cannot be arranged with 14-fold radial symmetry because the pore would be very large. Instead, we postulate that min K channels assemble in two stages. First, three monomers associate into a trimeric structure with 3-fold symmetry in which the TM helices form triple-stranded coiled coils. Each trimer has classic "knobs-into-holes" helix packing,

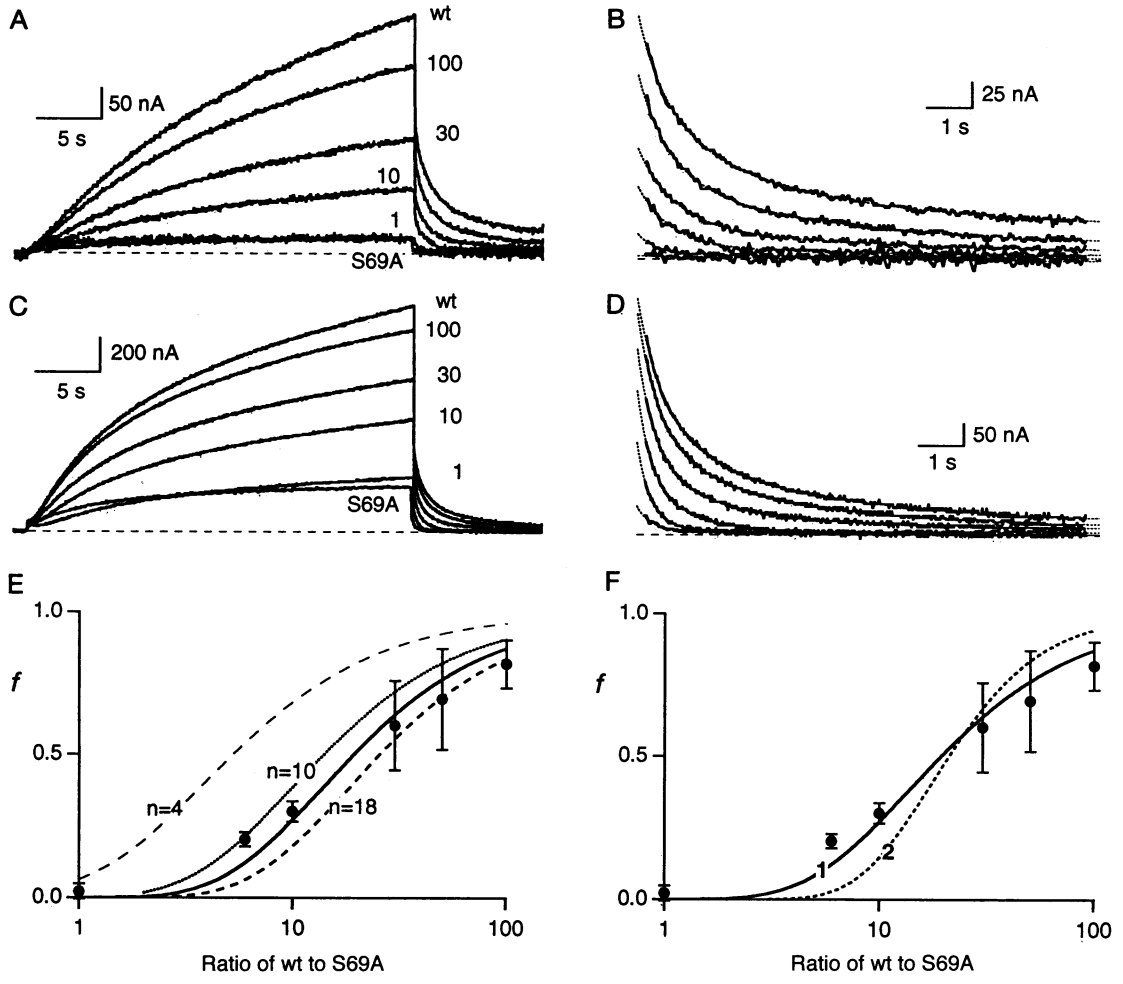

FIG. 3. Determination of subunit stoichiometry. Superimposed current records at −20 mV (*A*) and 20 mV (*C*) recorded from oocytes injected with mRNA at different ratios of wild-type to S69A mRNAs. The six traces represent wild-type mRNA alone (wt), coinjection of wild type and S69A mRNAs in proportions denoted as the ratio of wild type to S69A (100, 30, 10, 1), and S69A mRNA alone. Tail currents (*B* and *D*) were measured after a 30-s depolarizing step to −20 mV (*B*) or 20 mV (*D*) at −60 mV. Tail current traces are presented with double-exponential fits; note the change in kinetics apparent after test pulses to 20 mV. For all coinjections, the amount of wild-type mRNA was kept constant (5 ng) and the amount of S69A was varied. To determine the minimum number of subunits which form min K channels, the binomial distribution was applied (*E*). After depolarizations to −20 mV, the instantaneous tail currents at −60 mV were determined by fitting the traces with a sum of two exponentials and extrapolating back to the beginning of the tail pulse. These values were normalized to the tail current amplitude for oocytes injected with wild-type mRNA alone and plotted as a function of the ratio of wild type to S69A mRNA. Shown is a fit of the first term of the binomial expression $f = \{[\text{wild type}]/([\text{wild type}] + [\text{S69A}])\}^n$, where f = current amplitude of the coinjection mixture/current amplitude of wild type alone, [wild type] is the concentration of wild-type mRNA, [S69A] is the concentration of S69A mRNA, and n is the subunit stoichiometry. The data were best fit with a value of $n = 13.7$ (solid line). Also shown are relations for $n = 4$, 10, and 18 as indicated. *F* shows fits if 2 S69A subunits (labeled 2) are required for altered channel function, yielding a value of $n = 36$. Redrawn is the fit from *E* for 1 subunit required for altered channel function (labeled 1). All data points represent measurements from four oocytes and were gathered on the same day from the same batch of oocytes. Error bars are SD.

typical of coiled coils (23), and each of the subunits occupies an equivalent position.

The channel is hypothesized to form by the assembly of multiple trimers. Although the data are best fit if at least 14 subunits assemble to form min K channels, the packing of the helices is greatly improved if the channel is formed by five trimers, a "pentamer-of-trimers" with fivefold radial symmetry, in which the pore is formed from 5 internal subunits surrounded by 10 outer subunits (Fig. 4*A*). Because of the symmetry inherent in the trimers, each trimer subunit is equivalently capable of contributing to the formation of the inner ring. In this arrangement four phenylalanine residues

Table 2. Kinetics of wild type (WT) and coinjection mixtures for voltage commands to −20 mV

Channel	Activation			Deactivation		
	τ_{fast}, s	τ_{slow}, s	A_f	τ_{fast}, s	τ_{slow}, s	A_f
WT	10.0 ± 1.0	63 ± 2	0.14	0.5 ± 0.2	3.1 ± 0.1	0.50
1 WT + 0.01 S69A	10.7 ± 1.0	66 ± 3	0.12	0.5 ± 0.1	2.8 ± 0.2	0.50
1 WT + 0.1 S69A	10.5 ± 0.5	65 ± 3	0.13	0.5 ± 0.1	3.0 ± 0.1	0.55

Activation kinetics were examined by fitting a sum of two exponentials to the rising phase of the current trace at −20 mV. After repolarization to −60 mV, channel deactivation time course was fit by a sum of two exponentials. A_f is the relative contribution of the fast component; $n = 4$ for all measurements; errors are SD.

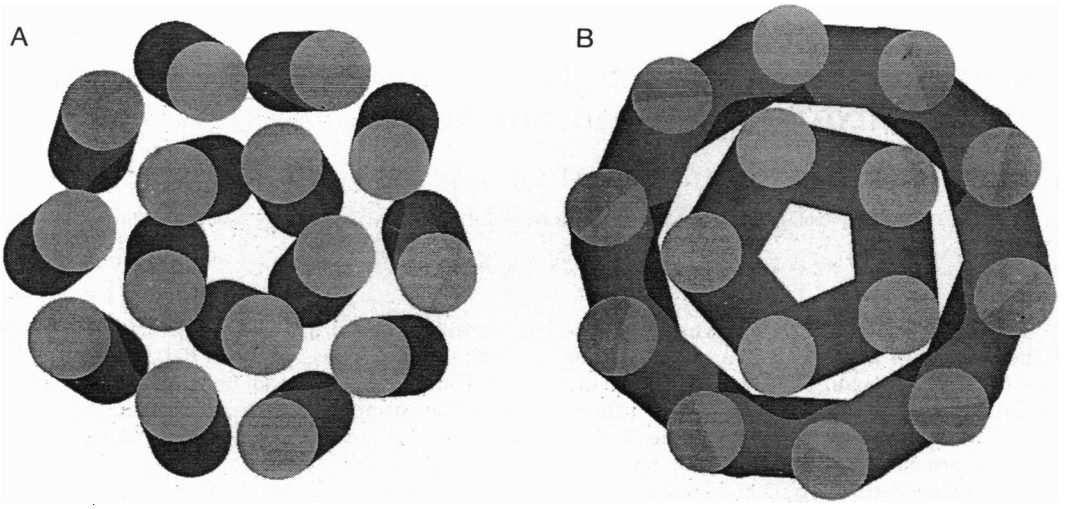

FIG. 4. min K channels formed from 15 subunits. (*A*) Five trimers of min K subunits associate into a "pentamer of trimers." Each trimer has a threefold degree of symmetry and the channel has a fivefold degree of symmetry. In this closed state, positively charged residues block access to the pore. (*B*) After depolarization, the channel undergoes a rearrangement such that the central five helices shift from a left-handed to a right-handed spiral around the axis of the pore. The positively charged residues are removed from the vicinity of the pore and the channel is capable of ion conduction.

(Phe-54, -55, -57, and -58) pack tightly together within each coiled coil and positively charged residues (Arg-68, Lys-70, and Lys-71) at the cytoplasmic end of the helices face away from the coiled coils and interact with lipid head groups. While the helical packing between subunits within the trimers is typical of coiled coils, the helical interaction between trimers is less typical. The channel is "closed" in this conformation because the central five helices are packed tightly together with positively charged residues near their termini inhibiting cation permeation. Membrane depolarization induces a rearrangement of the helices, as illustrated in Fig. 4*B*; in the open state all adjacent helices pack according to knobs-into-holes theory. The central five helices, those which form the pore, undergo the most dramatic movement during the closed → open conformational change, shifting from a left-handed to a right-handed spiral around the axis of the pore. Such a conformational change upon gating extends Phe-55 and Thr-59, which have been shown to affect ion selectivity (15), into the pore and orients charged residues (Glu-44 and Glu-73) toward the pore at either end of the helices. A more detailed model will be presented elsewhere.

We thank Dr. Steve Goldstein for the F55A mutant and for friendly and helpful interactions during the course of this work. We also acknowledge Wei-Bin Wu for *Xenopus* handling, oocyte preparation, and extreme patience. T.T. is supported in part by a Fulbright Scholarship. This work was supported by National Institutes of Health grants to J.M. and J.P.A.

1. Takumi, T., Ohkubo, H. & Nakanishi, S. (1988) *Science* **242,** 1042–1045.
2. Folander, K., Smith, J. S., Antanavage, J., Bennett, C., Stein, R. B. & Swanson, R. (1990) *Proc. Natl. Acad. Sci. USA* **87,** 2975–2979.
3. Pragnell, M., Snay, K. J., Trimmer, J. S., MacLusky, N. J., Naftolin, F., Kaczmarek, L. K. & Boyle, M. B. (1990) *Neuron* **4,** 807–812.
4. Sugimoto, T., Tanabe, Y., Shigemoto, R., Iwai, M., Takumi, T., Ohkubo, H. & Nakanishi, S. (1990) *J. Membr. Biol.* **113,** 39–47.
5. Busch, A. E., Kavanaugh, M. P., Varnum, M. D., Adelman, J. P. & North, R. A. (1992) *J. Physiol. (London)* **450,** 455–468.
6. Varnum, M. D., Busch, A. E., Bond, C. T., Maylie, J. & Adelman, J. P. (1993) *Proc. Natl. Acad. Sci. USA* **90,** 11528–11532.
7. Tempel, B. L., Papazian, D. M., Schwarz, T. L., Jan, Y. N. & Jan, L. Y. (1987) *Science* **237,** 770–775.
8. Christie, M. J., Adelman, J. P., Douglass, J. & North, R. A. (1989) *Science* **244,** 221–224.
9. Stuhmer, W., Ruppersberg, J. P., Schroter, K. H., Sakmann, B., Stocker, M., Giese, K. P., Perschke, A., Baumann, A. & Pongs, O. (1989) *EMBO J.* **8,** 3235–3244.
10. Butler, A., Wei, A., Baker, K. & Salkoff, L. (1989) *Science* **243,** 943–947.
11. Kubo, Y., Baldwin, T. J., Jan, Y. N. & Jan, L. Y. (1993) *Nature (London)* **362,** 127–133.
12. Bond, C. T., Pessia, M., Xia, X. M., Lagrutta, A., Kavanaugh, M. P. & Adelman, J. P. (1994) *Recept. Channels* **2,** 183–191.
13. Durell, S. R. & Guy, H. R. (1992) *Biophys. J.* **62,** 238–250.
14. Attali, B., Guillemare, E., Lesage, F., Honoré, E., Romey, G., Lazdunski, M. & Barhanin, J. (1993) *Nature (London)* **365,** 850–852.
15. Goldstein, S. A. N. & Miller, C. (1991) *Neuron* **2,** 403–408.
16. Tzounopoulos, T., Maylie, J. & Adelman, J. P. (1995) *Biophys. J.*, in press.
17. Liman, R. T., Tytgat, J. & Hess, P. (1992) *Neuron* **9,** 861–871.
18. MacKinnon, R. (1991) *Nature (London)* **350,** 232–235.
19. Fakler, B., Brandle, U., Bond, C., Glowatzki, E., Koenig, C., Adelman, J. P., Zenner, H.-P. & Ruppersberg, J. P. (1994) *FEBS Lett.* **356,** 199–203.
20. Shen, K. Z., Lagrutta, A., Davies, N. W., Standen, N. B., Adelman, J. P. & North, R. A. (1994) *Pflüger's Arch.* **426,** 440–445.
21. Adelman, J. P., Shen, K. Z., Kavanaugh, M. P., Warren, R. A., Wu, Y. N., Lagrutta, A., Bond, C. T. & North, R. A. (1992) *Neuron* **9,** 209–216.
22. Takumi, T., Moriyoshi, K., Aramori, I., Ishii, T., Oiki, S., Okada, Y., Ohkubo, H. & Nakanishi, S. (1991) *J. Biol. Chem.* **266,** 22192–22198.
23. Crick, F. H. C. (1953) *Acta Crystallogr.* **6,** 689–697.
24. Glowatzki, E., Fakler, G., Braendle, U., Rexhausen, U., Ruppersberg, J. P. & Fakler, B. (1995) *Proc. R. Soc. London B* **261,** 251–261.